



ZnFe₂O₄/MWCNTs composite with enhanced photocatalytic activity under visible-light irradiation

Cai-Hong Chen, Yan-Hui Liang, Wei-De Zhang*

Nano Science Research Center, School of Chemistry and Chemical Engineering, South China University of Technology, Guangzhou 510640, PR China

ARTICLE INFO

Article history:

Received 27 February 2010

Received in revised form 31 March 2010

Accepted 1 April 2010

Available online 20 April 2010

Keywords:

ZnFe₂O₄

Multi-walled carbon nanotubes

Visible light

Photocatalytic activity

ABSTRACT

Zinc ferrite/multi-walled carbon nanotubes (ZnFe₂O₄/MWCNTs) composite was prepared by a hydrothermal process and characterized by X-ray diffraction, transmission electron microscopy, and ultraviolet–visible diffusion reflectance spectroscopy. Compared with pure ZnFe₂O₄, the ZnFe₂O₄/MWCNTs composite exhibits stronger absorption in visible-light range and higher photocatalytic activity, with 99% degradation ratio of methylene blue after 6 h visible-light irradiation in the presence of H₂O₂. The enhanced photocatalytic activity is attributed to the strong interaction between ZnFe₂O₄ and MWCNTs which inhibits the recombination of photo-generated charge carriers, and the formation of highly active species •OH on the surface of MWCNTs. Therefore, more radicals are formed for degradation of the dye. The enhancing mechanism of the photocatalytic activity of ZnFe₂O₄ in the presence of MWCNTs is also discussed.

© 2010 Elsevier B.V. All rights reserved.

1. Introduction

Titanium dioxide (TiO₂) has been extensively studied as a photocatalyst for the degradation of organic pollutants [1]. However, the fatal drawback of TiO₂ is that it can only absorb UV light due to its wide band gap of 3.2 eV, which prevents it from utilizing solar energy efficiently. Other traditional visible-light photocatalysts (e.g. CdS, Fe₂O₃ and WO₃) bear drawbacks of either photocorrosion or low activity [2,3], which result in difficult application. In contrast, a great number of novel visible-light photocatalysts have been developed, such as BiVO₄ [4], CaBi₂O₄ [5], Bi₂WO₆ [6], Bi₂Fe₄O₉ [7]. Despite their absorption ability of visible light, most of these complex oxides were prepared by solid-state reaction under high temperature. They usually have small specific surface areas, which is liable to lower photocatalytic activities. Therefore, developing efficient methods to fabricate novel visible-light catalysts with excellent photocatalytic activity is urgently needed. Zinc ferrite (ZnFe₂O₄) is regarded as a promising visible-light photocatalyst with band gap of 1.9 eV that makes it possible to utilize solar energy [8]. In addition to its photochemical stability and low toxicity, ZnFe₂O₄ has been applied to degrade organic pollutants [9]. However, the poor quantum efficiency of ZnFe₂O₄ results in low photocatalytic activity. This can be improved by loading Ag on ZnFe₂O₄ surface [10]. However, the content of Ag is as high as 22.7%, which is impractical for application.

Recently, multi-walled carbon nanotubes (MWCNTs) have attracted great attention as supports for photocatalysts because of their large surface area, special aperture structure, high chemical stability and good electron conductivity. It has been reported that MWCNTs' supports for TiO₂ [11], WO₃ [12] and CdS [13] have greatly enhanced these oxides' activities. Inspired by these studies, the authors believe that it is worthwhile to attempt to add MWCNTs to ZnFe₂O₄ in the hope of improving its photocatalytic activity.

In this paper, ZnFe₂O₄ nanoparticles were coated on MWCNTs by a hydrothermal process. The effect of MWCNTs on photocatalytic activity was studied by degrading methylene blue (MB) dye under visible-light irradiation. Furthermore, the possible mechanism of the enhanced photocatalytic activity of ZnFe₂O₄ in the presence of MWCNTs was also discussed.

2. Experimental

2.1. Synthesis of the ZnFe₂O₄/MWCNTs

MWCNTs were prepared by catalytic chemical vapor deposition (CVD) of methane over Co/MgO catalysts [14]. The MWCNTs were further processed in a mixture of concentrated sulfuric acid (98%) and nitric acid (65%) with volume ratio at 1:2 [15].

All chemicals were purchased from local chemical agents with analytical grade and were used without further purification. For the synthesis of ZnFe₂O₄/MWCNTs, 5 mmol Zn(NO₃)₂·6H₂O and 10 mmol Fe(NO₃)₃·9H₂O were dissolved in 15 mL distilled water. 10 mg MWCNTs was added into the solution and sonicated for 10 min. An appropriate 6 M NaOH solution was added to the mixture until the pH reached 13. Then the volume of the solution was adjusted to 40 mL with distilled water. The mixture was stirred vigorously for 30 min and transferred into a 50 mL Teflon-lined stainless autoclave. The autoclave was sealed and maintained at 180 °C for 12 h. After that, the product was filtered, washed, and dried. The same procedure was applied to produce ZnFe₂O₄ without adding MWCNTs.

* Corresponding author. Tel.: +86 20 87114099.

E-mail address: zhangwd@scut.edu.cn (W.-D. Zhang).

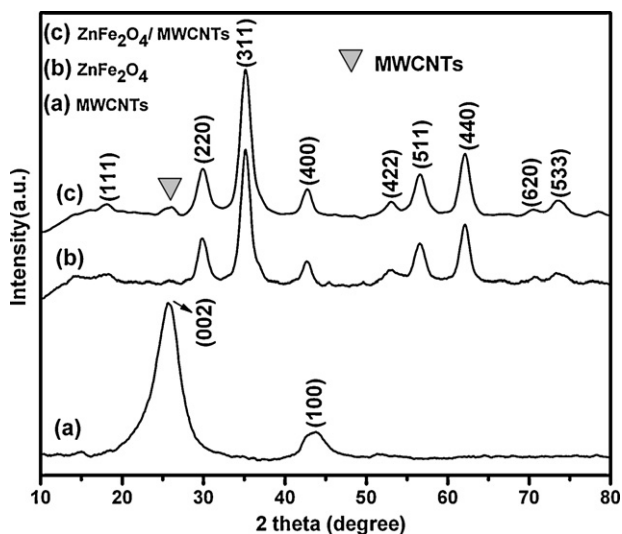


Fig. 1. XRD patterns of MWCNTs (a), ZnFe_2O_4 (b) and $\text{ZnFe}_2\text{O}_4/\text{MWCNTs}$ (c).

2.2. Characterization of the $\text{ZnFe}_2\text{O}_4/\text{MWCNTs}$

The XRD patterns were recorded using an X-ray diffractometer (X'Pert PRO, Philips, The Netherlands). The morphology of the samples was investigated by transmission electron microscopy (TEM, JEM-2010, JEOL Japan). The optical absorption of the powders was performed on a UV-vis spectrophotometer (U-3010, Hitachi, Japan). The Brunauer–Emmett–Teller (BET) surface area of the samples was determined using a specific surface area apparatus (ST-08, Beifen, China). The photoluminescence (PL) spectra of the samples were detected with a Fluorescence Spectrophotometer (F-4500, Hitachi, Japan).

2.3. Photocatalytic activity of the $\text{ZnFe}_2\text{O}_4/\text{MWCNTs}$

The photocatalytic reaction was conducted by adding 100 mg catalyst into 100 mL MB solution with concentration of 10 mg L^{-1} . To reach the balance of adsorption and desorption, the suspension was stirred in dark for 30 min. The light source was a 400 W metal halide lamp with a filter to cut off all wavelengths shorter than 420 nm. After adding 2.0 mL 30% H_2O_2 to the suspension, the lamp was turned on. Samples were taken out at regular time intervals and the changes of MB concentration were monitored using a UV-vis spectrometer (U-3010, Hitachi, Japan). The total organic carbon (TOC) in the solution before and after the photocatalytic reaction over the $\text{ZnFe}_2\text{O}_4/\text{MWCNTs}$ composite was determined by a TOC analyzer (Liqui, Germany). Furthermore, we investigated the ability of different photocatalysts to produce $\cdot\text{OH}$ by means of the terephthalic acid (TA)–fluorescence (FL) method [16] with a Fluorescence Spectrophotometer F-4500.

3. Results and discussion

3.1. XRD analysis of the $\text{ZnFe}_2\text{O}_4/\text{MWCNTs}$

XRD technique was used to investigate phase composition of the synthesized samples (Fig. 1). The peaks at 25.7° and 43.2° are attributed to the characteristic peaks of MWCNTs (Fig. 1a). The diffraction peaks in Fig. 1b correspond well to the reported values of spinel ZnFe_2O_4 (JCPDS 22-1012). As shown in Fig. 1c, the main peaks of the $\text{ZnFe}_2\text{O}_4/\text{MWCNTs}$ composite are in good accordance with pure ZnFe_2O_4 , which indicates that incorporation of a small amount of MWCNTs into ZnFe_2O_4 cannot lead to the change of its phase. One peak of MWCNTs at 25.7° is very low due to trivial amount of addition [17]. The other peak of MWCNTs at 43.2° might be overlapped by the main peak of spinel ZnFe_2O_4 at 42.8° , since they are so close.

3.2. TEM characterization of the $\text{ZnFe}_2\text{O}_4/\text{MWCNTs}$

The direct evidence of the formation of ZnFe_2O_4 nanoparticles on the surface of MWCNTs is given by TEM and HRTEM in Fig. 2. It can be seen that most of the MWCNTs have been covered with

ZnFe_2O_4 nanoparticles with an average size of 10 nm (Fig. 2a). Fig. 2b shows the HRTEM image of the composite. The lattice fringe spacings of nanocrystals are indexed as (400) and (311) planes of spinel ZnFe_2O_4 . In addition, ZnFe_2O_4 particles are firmly anchored on the surface of MWCNTs even after ultrasonic treatment. The strong combination of ZnFe_2O_4 and MWCNTs could be attributed to electrostatic interaction and chemical bonding through the functional groups on the surface of the modified MWCNTs [18]. As shown in Fig. 2c, most of the bare ZnFe_2O_4 nanoparticles are flaky and their size is about 15 nm. The ZnFe_2O_4 particles on the MWCNTs are obviously smaller than the bare ones, which could be attributed to the restriction effect of MWCNTs on the size of the attached nanoparticles [13,19], and they are also dispersed very well, resulting in a large surface area.

3.3. Diffuse reflectance UV-vis spectra of the $\text{ZnFe}_2\text{O}_4/\text{MWCNTs}$

The UV-vis absorption spectra of ZnFe_2O_4 , MWCNTs and $\text{ZnFe}_2\text{O}_4/\text{MWCNTs}$ are provided in Fig. 3. MWCNTs exhibit a very broad spectrum (Fig. 3a). The absorption of the $\text{ZnFe}_2\text{O}_4/\text{MWCNTs}$ composite (Fig. 3b) is stronger than that of the bare ZnFe_2O_4 particles (Fig. 3c) in the range of wavelength of 250–800 nm. In addition, the threshold of absorption band of the $\text{ZnFe}_2\text{O}_4/\text{MWCNTs}$ composite occurs at about 650 nm, which is a significant blue shift compared with the ZnFe_2O_4 (700 nm). The blue-shift absorption of the $\text{ZnFe}_2\text{O}_4/\text{MWCNTs}$ composite could be attributed to the quantum-size effects, which is consistent with the fact demonstrated by TEM.

3.4. Photocatalytic activity of the $\text{ZnFe}_2\text{O}_4/\text{MWCNTs}$

Photocatalytic activity was evaluated by measuring the degradation of MB. Fig. 4A shows the changes in the absorbance profiles of MB solution in the presence of $\text{ZnFe}_2\text{O}_4/\text{MWCNTs}$ composite and H_2O_2 under visible-light irradiation. The spectrum at $t=0$ h was taken on the starting solution of MB with a concentration of 10 mg L^{-1} (without H_2O_2). Four characteristic peaks (246, 291, 615, 664 nm) are observed, which are similar to those reported by Zhang et al. [20]. After stirring for 0.5 h, about 24% of the MB was adsorbed. As soon as H_2O_2 was added, the MB bands at 291 and 246 nm were masked by the strong absorption of H_2O_2 in the range of 185–300 nm [21]. With the irradiation time increasing, the peaks at 615 and 664 nm were reduced quickly. In addition, the original absorption maximum at 664 nm shifted to 660, 655, 651, 641, 620 nm after reaction for 1, 2, 3, 4 and 5 h, respectively. The blue shift of the absorption band indicates the photocatalytic degradation of MB [20,22]. The band at 620 nm became very weak and disappeared in 6 h, suggesting almost complete degradation of MB. Fig. 4B displays the photocatalytic degradation efficiency of MB monitored at 664 nm over the ZnFe_2O_4 , MWCNTs, $\text{ZnFe}_2\text{O}_4/\text{MWCNTs}$ composite and the mechanically mixed ZnFe_2O_4 and MWCNTs (with the same ratio of ZnFe_2O_4 to MWCNTs as in the $\text{ZnFe}_2\text{O}_4/\text{MWCNTs}$ composite) in the presence of H_2O_2 . Obviously, the $\text{ZnFe}_2\text{O}_4/\text{MWCNTs}$ composite exhibits the highest adsorption capacity and strongest photocatalytic activity among all the samples, with the MB degradation rate reaching 99% in 6 h. The TOC of this sample decreases from 15.23 to 1.49 mg L^{-1} , which confirms that 90% of MB is mineralized. Photocatalytic degradation of MB must have occurred here, because simple adsorption on the surfaces of the $\text{ZnFe}_2\text{O}_4/\text{MWCNTs}$ composite can only account for 24% of the decoloration. No appreciable degradation of the dye has been observed in the presence of neat MWCNTs or under direct photolysis for the same irradiation (data not shown). In the absence of any catalyst (only MB + H_2O_2), no obvious dye degradation is observed after 6 h. MWCNTs show great adsorption for MB but without distinct degradation of MB. It can be seen that the presence

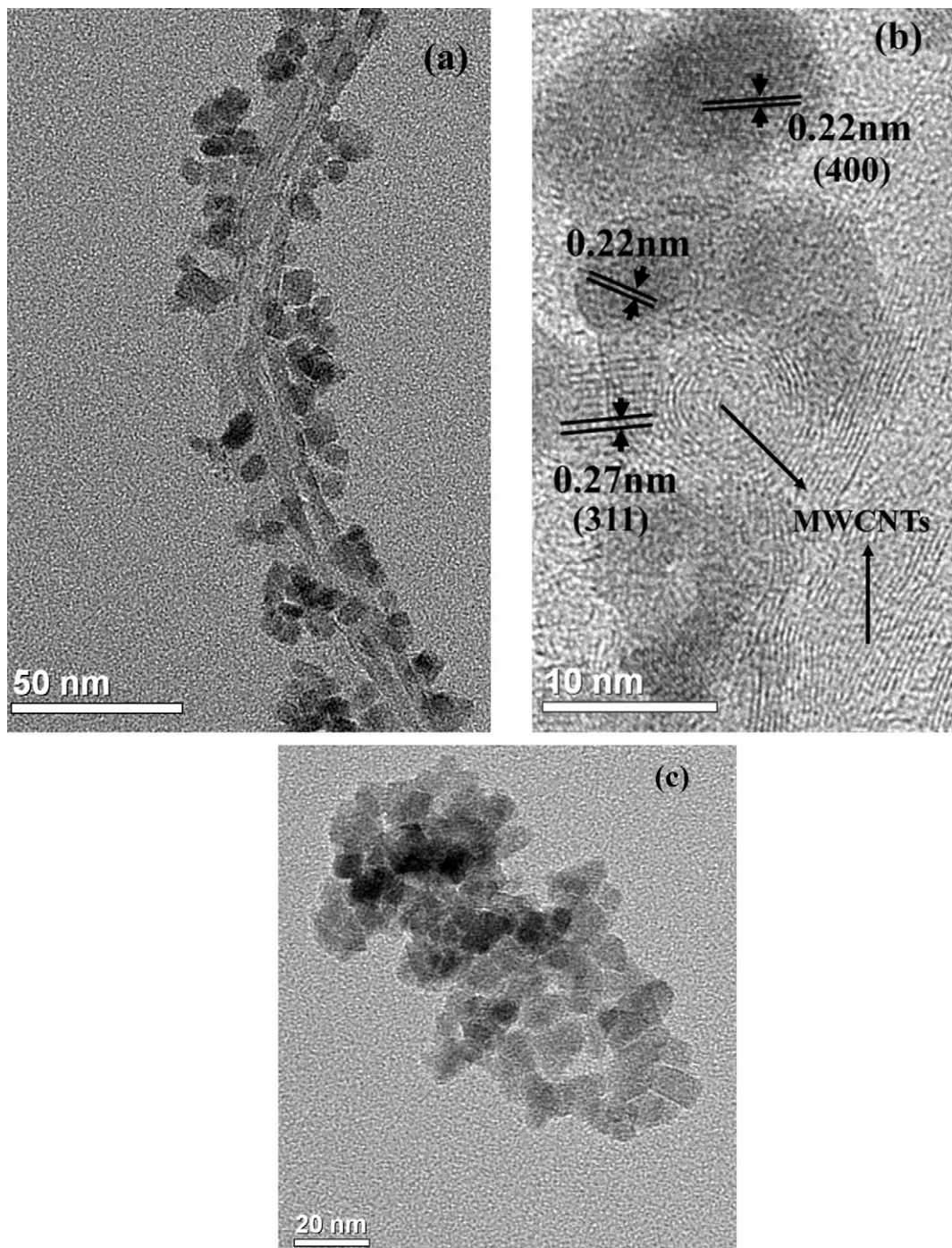


Fig. 2. TEM and HRTEM images of ZnFe₂O₄/MWCNTs (a, b) and ZnFe₂O₄ (c).

of MWCNTs enhanced the photocatalytic activity of ZnFe₂O₄ by comparing with the ZnFe₂O₄ and the mechanically mixed ZnFe₂O₄ and MWCNTs. No strong bonding between ZnFe₂O₄ and MWCNTs in the mechanical mixture intermits the transfer of electrons from ZnFe₂O₄ to MWCNTs. Moreover, ZnFe₂O₄ and MWCNTs are not uniformly distributed in the solution, and the enrichment of dye on the surfaces of MWCNTs cannot enhance its oxidation on the ZnFe₂O₄. Therefore, the photocatalytic activity of the mechanical mixture of ZnFe₂O₄ and MWCNTs is low. Although the degradation of MB over ZnFe₂O₄ and ZnFe₂O₄/MWCNTs in the presence of H₂O₂ happened in dark due to the formation of •OH from the decomposition of H₂O₂ on some transition metal oxides [23], they showed lower photocatalytic activity than those under irradiation respectively, which

demonstrates that the degradation reaction is definitely driven by visible light.

The BET surface area of the ZnFe₂O₄/MWCNTs composite is 72.9 m² g⁻¹, which is larger than that of the ZnFe₂O₄ powder (56.9 m² g⁻¹). The enlarged BET is attributed to the introduction of MWCNTs, which can improve the adsorption of MB.

The photoluminescence (PL) emission spectra are useful to disclose the migration, transfer, and recombination processes of the photo-generated electron-hole pairs in the semiconductor [24]. The PL emission mainly results from the recombination of the excited electrons and holes. In this study, the PL emission spectra of ZnFe₂O₄ and ZnFe₂O₄/MWCNTs were examined, as displayed in Fig. 5. One can see that ZnFe₂O₄ has a broad green emission peak at

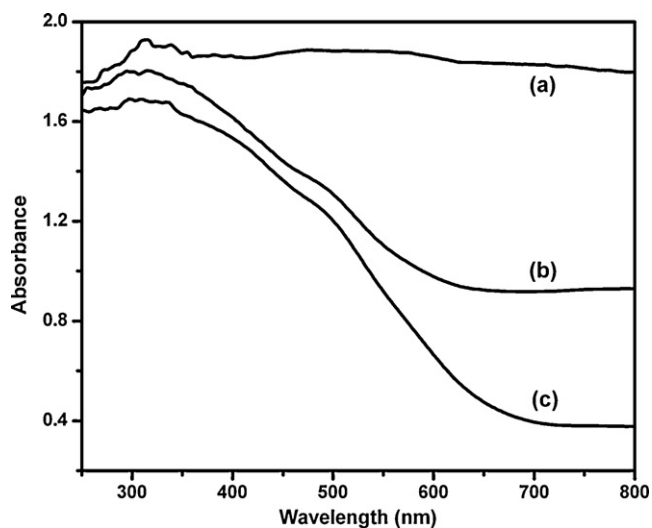


Fig. 3. UV-vis absorption spectra of (a) MWCNTs, (b) ZnFe₂O₄/MWCNTs and (c) ZnFe₂O₄.

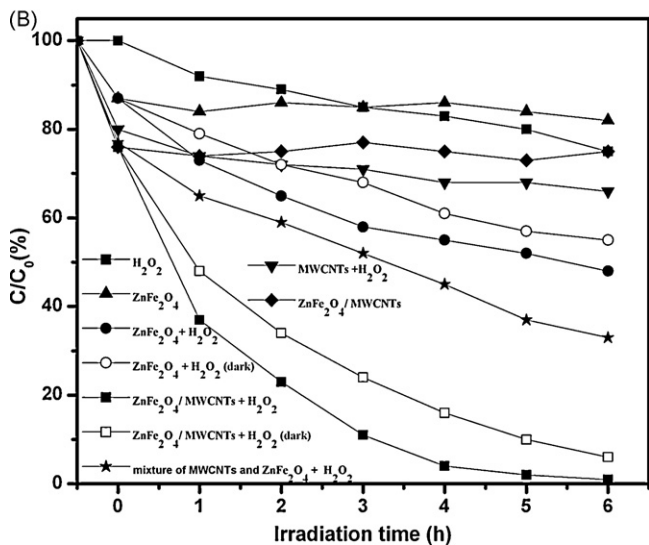
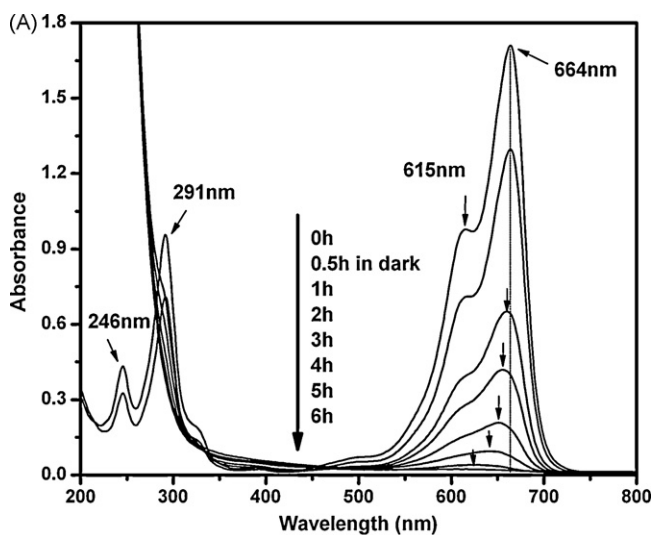


Fig. 4. (A) Absorption spectra of the (MB + H₂O₂ + ZnFe₂O₄/MWCNTs) composite solution taken at different reaction time. (B) Effect of different catalysts on photocatalytic decomposition of Methylene blue.

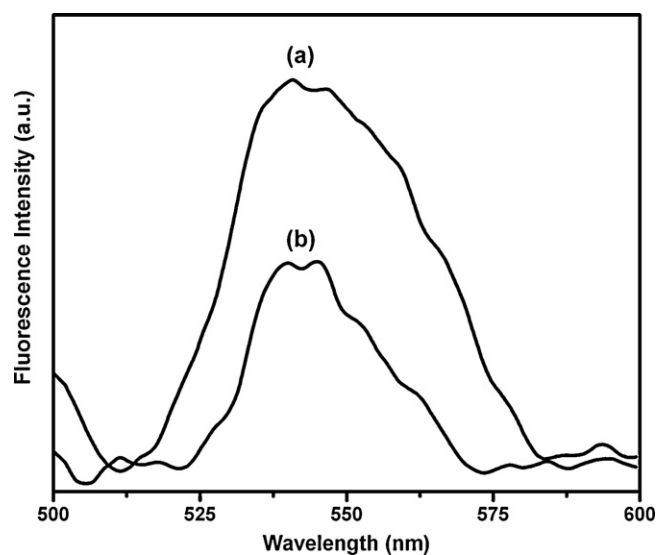


Fig. 5. The PL spectrum of ZnFe₂O₄ (a) and ZnFe₂O₄/MWCNTs (b) ($\lambda_{\text{ex}} = 315 \text{ nm}$).

538–547 nm, which is attributed to the recombination of holes and electrons in the valence band and conduction band. The PL intensity of the ZnFe₂O₄/MWCNTs composite is lower than that of pure ZnFe₂O₄, which shows that the recombination of photo-generated charge carriers is inhibited greatly, leading to the increase of highly reactive species for degradation of MB.

Fig. 6 represents linear relationship between the fluorescence intensity of 2-hydroxyterephthalic acid (TAOH) and the duration of visible-light irradiation. The concentration of $\cdot\text{OH}$ was estimated by comparing the fluorescence intensity to that of the known concentration of TAOH [25]. The formation rate of $\cdot\text{OH}$ ($r_{\cdot\text{OH}}$) of ZnFe₂O₄/MWCNTs in the presence of H₂O₂ under visible-light irradiation was about 4 times that of pure ZnFe₂O₄ under the same condition. Contrastively, in the case of ZnFe₂O₄ or ZnFe₂O₄/MWCNTs in the absence of H₂O₂, the $r_{\cdot\text{OH}}$ was extremely low. The ZnFe₂O₄/MWCNTs in the presence of H₂O₂ in dark shows higher $r_{\cdot\text{OH}}$ than the mixture of ZnFe₂O₄ and MWCNTs. These experimental results indicate that the surface condition of ZnFe₂O₄/MWCNTs is more favorable than that of pure ZnFe₂O₄ or the mixture of ZnFe₂O₄ and MWCNTs in the formation of $\cdot\text{OH}$ for oxidizing the dye in the system, which is consistent with the photocatalytic performance discussed above.

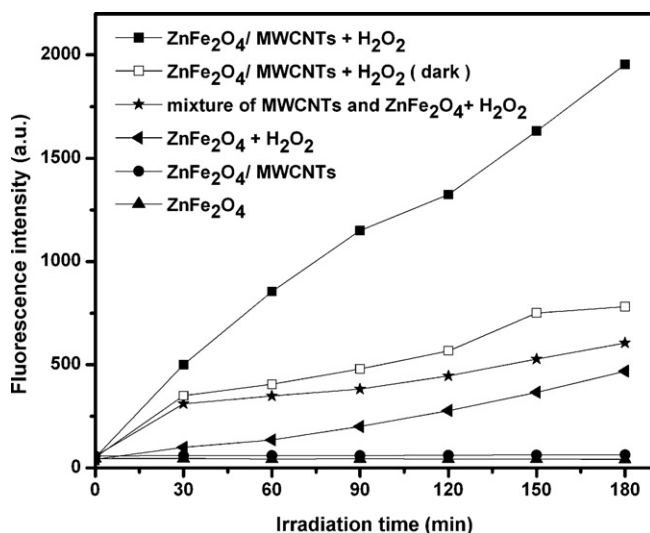


Fig. 6. The changes of the fluorescence intensity of 2-hydroxyterephthalic acid at 425 nm under various conditions.

The enhanced photocatalytic activity of the ZnFe₂O₄/MWCNTs for degradation of MB presumably results from the following reasons. Firstly, MWCNTs improve the absorption of dye and H₂O₂ due to their large surface area and special aperture structure. Secondly, when visible light is illuminated on the ZnFe₂O₄ nanocrystalline, electrons are excited from the valence band to the conduction band. Then, the excited electrons transfer from ZnFe₂O₄ to the MWCNTs, thus the recombination of electron-hole pairs are effectively hindered [26]. As a result, more photo-generated holes can react with adsorbed water to form •OH, which is available to promote the decomposition of MB. Thirdly, H₂O₂ can act as an effective electron scavenger to form •OH on the surface of MWCNTs [27], which not only enhances oxidation ability but also fleetly reduces electronic accumulation on the surface of MWCNTs. Therefore, the ZnFe₂O₄/MWCNTs composite exhibits enhanced photocatalytic activity under visible-light irradiation in the presence of H₂O₂.

4. Conclusion

The ZnFe₂O₄/MWCNTs composite was prepared by hydrothermal method. This composite shows higher ability of visible-light absorption and lower PL intensity than that of pure ZnFe₂O₄. The presence of MWCNTs improved the photocatalytic activity of ZnFe₂O₄ significantly. On the basis of PL spectra and •OH measurement, the enhancing mechanism for photocatalytic activity of the ZnFe₂O₄/MWCNTs composite is probably attributed to effective separation of electron-hole pairs and the formation of •OH. This study is believed to be useful not only for understanding the photocatalytic mechanism but also for developing effective photocatalyst in pollutant decomposition.

Acknowledgement

This work was supported by the National Natural Science Foundation of China under grant No. 20601009 and 20773041.

References

- [1] A.L. Linsebigler, G.Q. Lu, J.T. Yates, *Chem. Rev.* 95 (1995) 735–758.
- [2] G.C. De, A.M. Roy, S.S. Bhattacharya, *Int. J. Hydrogen Energy* 21 (1996) 19–23.
- [3] D.W. Hwang, J. Kim, T.J. Park, J.S. Lee, *Catal. Lett.* 80 (2002) 53–57.
- [4] A. Kudo, K. Ueda, H. Kato, I. Mikami, *Catal. Lett.* 53 (1998) 229–230.
- [5] J.W. Tang, Z.G. Zou, J.H. Ye, *Angew. Chem. Int. Ed.* 43 (2004) 4463–4466.
- [6] J.W. Tang, Z.G. Zou, J. Yin, J.H. Ye, *Catal. Lett.* 92 (2004) 53–56.
- [7] Q.J. Ruan, W.D. Zhang, *J. Phys. Chem. C* 113 (2009) 4168–4173.
- [8] S.B. Li, G.X. Lu, *New. J. Chem.* 16 (1992) 517–519.
- [9] J.X. Qiu, C.Y. Wang, M.Y. Gu, *Mater. Sci. Eng. B* 112 (2004) 1–4.
- [10] X.B. Cao, L. Gu, X.M. Lan, C. Zhao, D. Yao, W.J. Sheng, *Mater. Chem. Phys.* 106 (2007) 175–180.
- [11] Y. Ying, J.C. Yu, C.Y. Chan, Y.K. Che, J.C. Zhao, L. Ding, W.K. Ge, P.K. Wong, *Appl. Catal. B Environ.* 61 (2005) 1–11.
- [12] S. Wang, X.L. Shi, G.Q. Shao, X.L. Duan, H. Yang, T.G. Wang, *J. Phys. Chem. Solids* 69 (2008) 2396–2400.
- [13] L.L. Ma, H.Z. Sun, Y.G. Zhang, Y.L. Lin, J.L. Li, E.K. Wang, Y. Yu, M. Tan, J.B. Wang, *Nanotechnology* 19 (2008) 115709.
- [14] E. Flahaut, A. Peigney, C. Laurent, A. Rouseet, *J. Mater. Chem.* 10 (2000) 249–252.
- [15] H.W. Goh, S.H. Goh, G.Q. Xu, K.P. Pramoda, W.D. Zhang, *Chem. Phys. Lett.* 379 (2003) 236–241.
- [16] K. Ishibashi, A. Fujishima, T. Watanabe, K. Hashimoto, *Electrochem. Commun.* 2 (2000) 207–210.
- [17] H. Wang, H.L. Wang, W.F. Jiang, *Chemosphere* 75 (2009) 1105–1111.
- [18] Q. Zhang, M.F. Zhu, Q.H. Zhang, Y.G. Li, H.Z. Wang, *Mater. Chem. Phys.* 116 (2009) 658–662.
- [19] P. Chen, X. Wu, J. Lin, K.L. Tan, *J. Phys. Chem. B* 103 (1999) 4559–4561.
- [20] T.Y. Zhang, T. Oyama, A. Aoshima, H. Hidaka, J.C. Zhao, N. Serpone, *J. Photochem. Photobiol. A* 140 (2001) 163–172.
- [21] A. Lopez, A. Bozzi, G. Mascolo, J. Kiwi, *J. Photochem. Photobiol. A* 156 (2003) 121–126.
- [22] W.X. Zhang, Z.H. Yang, X. Wang, Y.C. Zhang, X.G. Wen, S.H. Yang, *Catal. Commun.* 7 (2006) 408–412.
- [23] C.C. Wong, W. Chu, *Environ. Sci. Technol.* 37 (2003) 2310–2316.
- [24] J.W. Tang, Z.G. Zou, J.H. Ye, *J. Phys. Chem. B* 107 (2003) 14265–14269.
- [25] T. Hirakawa, Y. Nosaka, *Langmuir* 18 (2002) 3247–3254.
- [26] W.D. Zhang, L.C. Jiang, J.S. Ye, *J. Phys. Chem. C* 113 (2009) 16247–16253.
- [27] J.G. Yu, X.X. Yu, B.B. Huang, X.Y. Zhang, Y. Dai, *Cryst. Growth Des.* 9 (2009) 1474–1480.